A Novel Method for Transverse Beam-Coupling Impedance Measurements in Particle Accelerator Devices Using the Bead-Pull Method

Chiara Antuono, Leonardo Sito, Eleonora Calzone, D. el Dali, Mauro Migliorati, Andrea Mostacci, Francesco Fienga, *Member, IEEE*, Vincenzo Romano Marrazzo, Giovanni Breglio, G. Rumolo, and Carlo Zannini

***Abstract*— In high-energy particle accelerators, circulating particle beams with high intensity interact electromagnetically with their surroundings (i.e., metallic vacuum chambers of various geometries). These electromagnetic interactions, which are typically described through the concept of beam-coupling impedance, can represent a serious issue in terms of stability of the particle beam and heating on the accelerator structures. It is therefore crucial to account for beam-coupling impedance through simulations and measurements during the design phase of an accelerator component. However, standard methods used in the accelerator field have known limitations due to the perturbations that they induce in the device geometry. Thus, the bead-pull method, which is a possible alternative approach, is presented in this study. The longitudinal beam-coupling impedance measurement technique is introduced, and it is further developed for novel use in transverse impedance measurements.**

***Index Terms*— Bead-pull method, beam-coupling impedance, radio-frequency (RF) cavity, Slater theorem, transverse impedance.**

I. Introduction

RESEARCH in energy physics uses particle accelerator machines which are ultrahigh-vacuum metallic chambers hosting an ultrarelativistic beam of charged particles. The trend for future high-energy particle accelerator physics is moving toward increasing the energy and the intensity (i.e., the number of circulating particles in the machine) of the beams [1], [2]. Going toward this goal, some physical phenomena start becoming more relevant and potentially detrimental [3]; one of the main issues is given by the interaction between the electromagnetic field irradiated by the traveling particles and the metallic pipes containing the beam. This complex interaction is synthetically described through the concept of beam-coupling impedance [4]. More specifically, the beam-coupling impedance contribution can be separated into two components, one associated with the longitudinal direction (the beam propagation direction) and the other associated with the transverse plane (orthogonal to the beam propagation direction). These components can be responsible for beam-induced heating deposition [5] on the accelerator devices and beam stability and quality degradation [6]. Both the aspects are undeniably critical for ensuring proper operation and enhancing the overall performance of the accelerators, and this explains the need for: 1) accurately monitoring the device temperature during operation [7] and 2) quantifying the impedance contribution of an accelerator device both during its design phase and in postmortem scenarios.

In the context of measuring the beam-coupling impedance, the ideal approach involves the excitation of the device using the beam itself [6]. However, this may not always be feasible. In such cases, alternative methods such as simulations or bench measurements [8] become necessary.

The most commonly used bench methods, i.e., the coaxial-wire and the coaxial probe methods, have notable limitations. In the coaxial-wire method [9], [10], a wire is stretched through the structure and it is excited with a current pulse (which mimics the beam passage). The stretched wire perturbs the electromagnetic boundary conditions of the original design, potentially resulting in inaccurate results, as demonstrated and documented in [11] and [12]. On the other hand, wireless methods, such as the coaxial probe technique, introduce less perturbations in the boundary conditions of the structure but they do not supply all the information needed to quantify the beam-coupling impedance.

An alternative method, typically used in the radio-frequency (RF) community for fine tuning of modes in an electromagnetic resonant cavity [13], [14], is the bead-pull method. In the context of accelerator physics, the bead-pull method has been so far used only for measurements of longitudinal

Received 13 June 2024; revised 6 August 2024; accepted 20 August 2024. Date of publication 12 September 2024; date of current version 27 September 2024. The Associate Editor coordinating the review process was Dr. Tae-Weon Kang. *(Corresponding authors: Chiara Antuono; Leonardo Sito.)*

Chiara Antuono and Eleonora Calzone are with the Physics Department, University of Rome "La Sapienza," 00185 Rome, Italy, and also with the European Organization for Nuclear Research (CERN), 1211 Geneva, Switzerland (e-mail: chiara.antuono@cern.ch; eleonora.calzone@gmail.com).

Leonardo Sito, Francesco Fienga, Vincenzo Romano Marrazzo, and Giovanni Breglio are with the Dipartimento di Ingegneria Elettrica e dell Tecnologie dell'Informazione, University of Naples Federico II, 80138 Naples, Italy, and also with the European Organization for Nuclear Research (CERN), 1211 Geneva, Switzerland (e-mail: leonardo.sito@cern.ch, francesco.fienga@unina.it; vincenzoromano.marrazzo@unina.it; breglio@unina.it).

D. el Dali, G. Rumolo, and Carlo Zannini are with the European Organization for Nuclear Research (CERN), 1211 Geneva, Switzerland (e-mail: daliaeldali97@gmail.com; giovanni.rumolo@cern.ch; carlo.zannini@cernc.ch).

Mauro Migliorati and Andrea Mostacci are with the Department of Basic and Applied Sciences for Engineering, University of Rome "La Sapienza," 00185 Rome, Italy, and also with the European Organization for Nuclear Research (CERN), 1211 Geneva, Switzerland (e-mail: mauro.migliorati@uniroma1.it; andrea.mostacci@uniroma1.it).

Digital Object Identifier 10.1109/TIM.2024.3458042

beam-coupling impedance. In addition to the consolidation of the bead-pull method as a longitudinal impedance bench measurement technique, the novelty of this work is the extension to transverse impedance measurements which will be showcased and benchmarked with simulations. To move toward this goal, a portable and general-purpose bead-pull setup will be presented as well. This article starts with a background section explaining the concepts and definitions of the beam-coupling impedance. It follows a review of the standard bench measurement techniques underlying their limitations with respect to the specific device we are using for the benchmark (a pillbox cavity). There is a section dedicated to the theory of the standard bead-pull method, in which the setup implemented will be showcased. Finally, the idea of the extension of the method to transverse measurements will be explained and the resulting benchmark will be shown and discussed.

II. Wakefields and Beam-Coupling Impedance

When a beam of charged particles travels in the vacuum chamber of a particle accelerator, it is subject to external electromagnetic fields (typically produced by magnets for bending or focusing and RF cavities for acceleration). However, the particles are themselves source of an electromagnetic field that can act directly on other particles or indirectly through scattering on the walls of the vacuum chamber. In high-energy physics accelerators, the particles are traveling at ultrarelativistic speed. Then, the field resulting from the interaction with the vacuum chamber is completely behind the particle that generated it. For this reason, these fields are commonly called wakefields (WFs) [15].

As the beam intensity increases, the WFs become stronger in amplitude and they can interact with the trailing bunches of particles disturbing their motion. More specifically, due to the Lorentz force, the fields can induce kicks on the particles with the undesired effects of deflecting the beam, causing energy loss, increasing the beam spot-size, and, ultimately, triggering instabilities [6], [15]. All these effects can cause a severe degradation of the performance of the accelerator. Moreover, the WFs can be the cause for electromagnetic power deposition on the accelerator component leading to a phenomenon called beam-induced heating [5], [16], [17]. For describing these phenomena, it is usually more convenient to work with a simplified description of the WFs which considers integrated effects.

We consider an idealized scenario where particles move all at the same speed, that is, the speed of light (c). A particle (with charge q_s) enters an accelerator device (which, for these analyses, can be schematically considered either as a cavity-like structure or as a pipe with a certain cross-section) moving in the $\hat{z}$-direction. This source particle generates a time-varying electromagnetic field at the point in space $\mathbf{r} = (x, y, z)$ $(\mathbf{E}(\mathbf{r}, t), \mathbf{B}(\mathbf{r}, t))$ in the structure located all behind it. The momentum change in a "test" particle (with charge q_t) entering the cavity at a certain distance (s) behind the source particle would be [4]

$$\Delta\mathbf{p}_t = q_t \int_{-\infty}^{+\infty} dt\big[\mathbf{E}(\mathbf{r}_t(t), t) + c\hat{z} \times \mathbf{B}(\mathbf{r}_t(t), t)\big]. \quad (1)$$

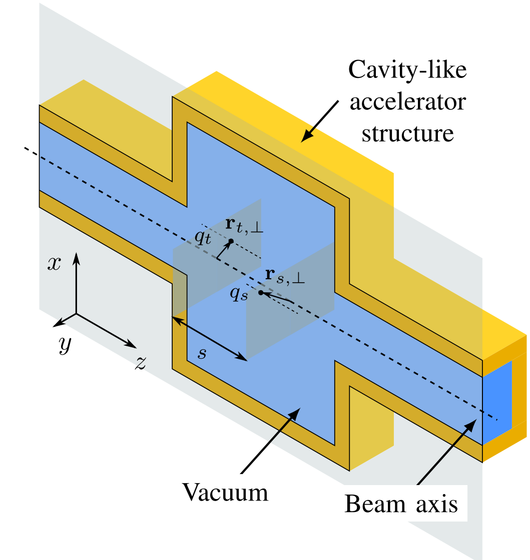

Fig. 1. Cavity-like accelerator structure cut-view. The source and test charges (q_s and q_t, respectively) are traveling at the speed of light spaced at a constant distance s. Their positions are given by the vectors $\mathbf{r}_s = (x_s, y_s, ct) = (\mathbf{r}_{s,\perp}, \mathbf{r}_{s,\parallel})$ and $\mathbf{r}_t = (x_t, y_t, ct - s) = (\mathbf{r}_{t,\perp}, \mathbf{r}_{t,\parallel})$.

The considered scenario is schematically depicted in Fig. 1. The wake function is defined as

$$\boldsymbol{w}(\mathbf{r}_{s,\perp}, \mathbf{r}_{t,\perp}, s) = \frac{c}{q_s q_t}\Delta\mathbf{p}_t. \quad (2)$$

The wake function is usually split into a longitudinal component (w_l) and a transverse component ($\boldsymbol{w}_t$)

$$w_l = -\frac{c}{q_s q_t}\Delta p_{t,z} = -\frac{c}{q_s}\int_{-\infty}^{\infty} dt\, E_z(\mathbf{r}_t(t), t) \quad (3)$$

$$\boldsymbol{w}_t = \frac{c}{q_s q_t}\Delta\mathbf{p}_{t,\perp} \quad (4)$$

where the longitudinal wake function is usually taken with a minus sign so that a positive value is associated with energy loss of the test particle. Moreover, since the longitudinal beam-coupling impedance only depends on the longitudinal component of the electric field, it is evident from (3) that only TM modes in the structure will contribute to it.

The longitudinal and transverse wake functions are linked through their transverse space derivatives, thanks to the Panofsky–Wenzel theorem [18]

$$-\frac{\partial}{\partial z}\boldsymbol{w}_t = \nabla_t w_l. \quad (5)$$

The wake functions represent a description of the WFs in the time domain; however, in a number of practical applications, it is more convenient to have a description in the frequency domain. Thus, the Fourier transform of the wake function is the quantity called beam-coupling impedance

$$Z_l = \frac{1}{c}\int_{-\infty}^{+\infty} ds\;\, w_l e^{j\omega s/c} \quad (6)$$

$$\mathbf{Z}_t = -\frac{j}{c}\int_{-\infty}^{+\infty} ds\;\, \boldsymbol{w}_t e^{j\omega s/c} \quad (7)$$

where j is the imaginary unit and $\omega = 2\pi f$, with f being the frequency. The longitudinal and transverse beam-coupling impedances are related through the Panofsky–Wenzel theorem [4]

$$\omega \mathbf{Z}_t = c\nabla_\perp Z_l. \quad (8)$$

In the context of impedance bench measurements, it is more practical to measure the longitudinal beam-coupling impedance, and through the Panofsky–Wenzel theorem, it is possible to evaluate the transverse impedance.

When the major impedance contribution is due to modes resonating in the structure (and this is the case of the pillbox cavity considered in this article), it can be helpful to write the beam-coupling impedance (both longitudinal and transverse) with an analytical resonator model [19]

$$Z(\omega) = \frac{R_s}{1 + jQ\left(\frac{\omega}{\omega_R} - \frac{\omega_R}{\omega}\right)} \quad (9)$$

where R_s is the shunt impedance [20], Q is the quality factor, and ω_R is the angular resonant frequency. It is therefore possible to characterize a cavity-like structure in terms of beam-coupling impedance considering these three parameters for each mode excited in the cavity.

The beam-coupling impedance concept is typically used in particle accelerator physics to describe both some longitudinal and transverse beam instabilities [21], [22], [23] and for accounting for heating of devices due to power dissipated by the beam [24]. This explains the need for an accurate estimation of the beam-coupling impedance and the demand for improved bench measurement techniques like the one that will be presented in this article.

III. Standard Measurement Techniques

Although analytical computations or numerical simulations are widely used, in most cases, they are not enough to properly characterize the device under test (DUT) particularly when dealing with complex geometries or unknown material properties within the relevant frequency range. Moreover, measurements are crucial both prior to device installation (to verify conformity) and after installation, especially in cases where operational issues arise during accelerator operation [25], [26].

The standard bench measurement techniques to measure the beam-coupling impedance of accelerator devices are: 1) the wire method [9] and 2) the probe method. However, both of them present limitations in some scenarios. A detailed description is provided in the following paragraphs, where these methods are tested on a very simple DUT which still underlines their criticalities. Moreover, the use of the bead-pull method for the evaluation of the solely longitudinal beam impedance (already present in [8] and [27]) will be further treated in Section IV.

A. Wire Method

The stretched wire method is widely used for the longitudinal and transverse beam-coupling impedance measurements [9]. The method has been developed, improved, and tested in several decades [10], [28], [29], [30] proving to be extremely effective in some scenarios with complex devices

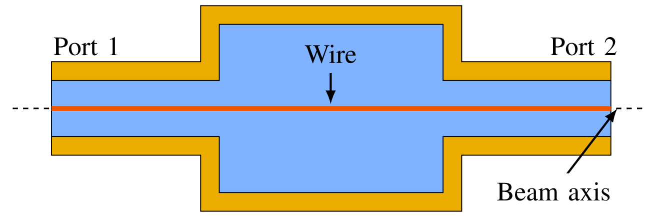

Fig. 2. Wire method setup: cross section of a cavity-like structure with the stretched metallic wire (typically copper) along the beam axis.

such as kickers [31], [32], [33], [34]. Typically, the DUT is closed by two metallic hollow flanges and a copper wire is stretched along the axis of the DUT. Both the ends of the wire are then connected to a vector network analyzer (VNA), as illustrated in Fig. 2.

The field excitation generated by the relativistic particle beam passing through the DUT, especially its longitudinal pulsed current distribution, can be approximated by a current pulse (with identical temporal behavior) flowing through the wire aligned with the beam axis.

The longitudinal beam-coupling impedance can be related to the measured scattering parameters through the following general formula [9]:

$$Z_l = -Z_c \ln \frac{S_{21}^{\mathrm{DUT}}}{S_{21}^{\mathrm{REF}}}\left[1 + \frac{\ln S_{21}^{\mathrm{DUT}}}{\ln S_{21}^{\mathrm{REF}}}\right] \quad (10)$$

where S_{21}^{DUT} is the transmission scattering parameter of the DUT measured in the configuration shown in Fig. 2. The S_{21}^{REF} is the reference transmission scattering parameter. It refers to the case in which the scattering parameters are measured or assessed on the DUT when its impedance contribution is removed (i.e., a wire and beam-pipe ensemble, resembling a TEM coaxial line). The Z_c is the characteristic impedance of this TEM coaxial line.

This method presents some critical aspects: 1) it is not always possible to perform a reference measurement and 2) the introduction of a metallic conductor along the device axis alters the electromagnetic boundary conditions of the original DUT. More specifically, the insertion of a second conductor (the wire) other than the cavity walls creates a nonsimply connected geometry which allows TEM wave propagation. This TEM propagation should not have been present in the cavity when excited by the particle beam alone. This has the implication of introducing a detuning/shift of the frequency of the impedance resonances with respect to the expectations. Moreover, it could also introduce some additional losses leading to incorrect magnitude of impedance resonances and incorrect evaluation of the quality factors. This is particularly detrimental below the cutoff frequency of the beam pipe of the device, as previously demonstrated in [11]. For these reasons, the wire method provides inaccurate results for resonant structures.

Once the longitudinal impedance has been measured, the wire method can be used to determine the transverse impedance by applying the Panofsky–Wenzel theorem [29]. However, this requires offsetting the wire with respect to the beam chamber axis. From a mechanical point of view, for each specific device, there is the need to develop a moving

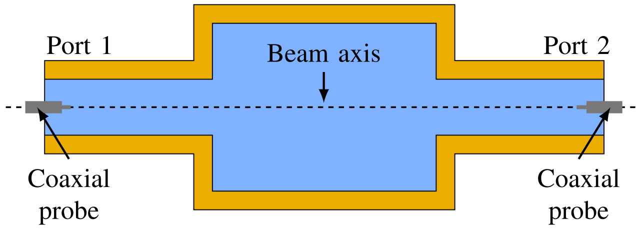

Fig. 3. Probe method setup: cross-section of a cavity-like structure with the electric probes inserted along the beam axis.

support system to implement the offset of the wire. This can be challenging and expensive.

B. Probe Method

The probe method relies on a transmission measurement conducted by inserting two electric probes (ending with straight pins) or magnetic probes (ending with loops) in the DUT closed with hollow flanges (see Fig. 3). The probes are connected to the two ports of a VNA and oriented in such a way as to excite TM modes.

The intrinsic resonances of the device typically remain unchanged in frequency when the penetration of the probes in the device varies. This is true only if the probes' position does not allow excessive coupling with the signal and there is no relevant geometric modification. Therefore, it is crucial to conduct measurements in an under-coupled configuration with the excitation probes, monitoring not only the transmission parameters but also the reflection scattering parameters [19].

This technique, through the excitation of TM modes in the structure, enables the identification of the intrinsic resonances contributing to the longitudinal impedance. This is a major limitation for the comprehensive characterization of the beam-coupling impedance unless these measurements are coupled with simulations. Efforts are being made to develop a wireless method using the probe excitation for the beam-coupling impedance measurements [35].

C. Characterization of the DUT

As already said, the previously shown methods can present some limitations when measuring resonant structures. To showcase these limitations, in this section, we present the DUT of our interest and the information extracted with the wire and probe methods compared with simulations. The DUT considered is a circular pillbox cavity, shown schematically in Fig. 4.

The results of measurements and simulations are shown in Fig. 5 and summarized in Table I. The simulations are performed using the WF solver of CST Studio Suite [36] which provides the beam-coupling impedance simulating a particle beam traveling along the DUT, and therefore it provides the appropriate excitation.

When comparing expected values from WF simulations and the two standard bench measurement techniques, their limitations are evident. In the case of the wire method, as already discussed at the end of Section III-A, the resonant frequency is shifted by almost 11% with respect to the expectation. Moreover, also R_S and Q show discrepancies

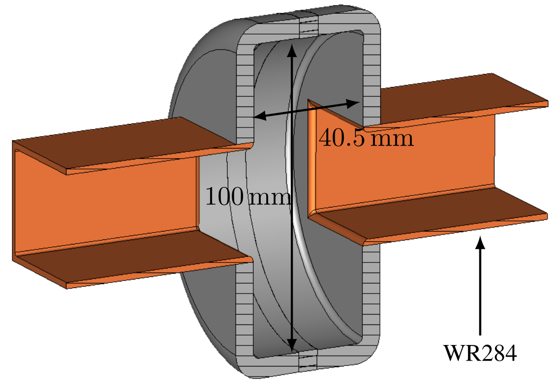

Fig. 4. Cross section of the 3-D model of the DUT. The pillbox cavity has an inner radius of 50 mm and a length of 40.5 mm. It is terminated with two copper WR284 waveguides.

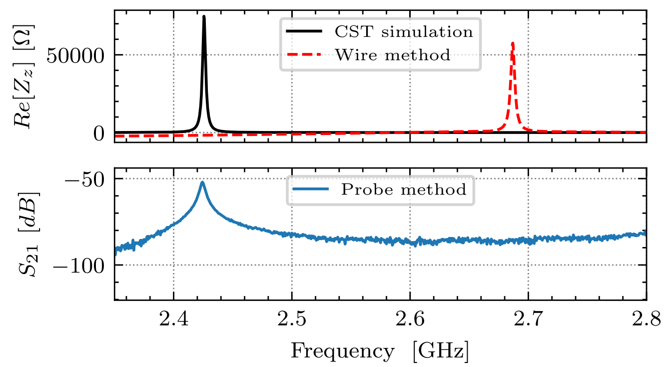

Fig. 5. Characterization of the DUT. Top, the real part of the longitudinal beam-coupling impedance as a function of frequency with a comparison between the wire method and a CST WF simulation. Bottom, the transmission scattering parameter obtained through a probe measurement. All the measurements were performed using a standard short–open–load–through (SOLT) two-port calibration. The reference planes were at the end of the cables.

TABLE I
COMPARISON BETWEEN THE METHODS AND SIMULATION

	f_R [GHz]	R_S [kΩ]	Q
Wire	2.686	57.4	650
Probes	2.424	-	770
Simulation	2.425	75	777

(23% and 16%, respectively). In the case of probe method, the transmission scattering parameter shows accurate values of resonant frequency and Q (less than 0.1% and less than 1%, respectively). However, the biggest limitation is given by the incomplete information about R_S that cannot be estimated with this method.

IV. BEAD-PULL METHOD

A. Theory and Concept: The Slater Theorem

The bead-pull method relies on Slater's small perturbation theory [37], [38], which states that when a resonant cavity is perturbed by a small bead, whether metallic or dielectric, the resonant frequency varies from its unperturbed value. The relative frequency shift is proportional to the combination of the squared amplitudes of the electrical and magnetic fields at the location of the bead. The frequency shift due to the material medium perturbation can be written as follows [19]:

$$\frac{\Delta f}{f_R} \approx \frac{\int_{\Delta V}\left[\mu_r\mu_0|\mathbf{H_0}|^2 - \epsilon_r\epsilon_0|\mathbf{E_0}|^2\right]dV}{\int_{V_0}(\mu_r\mu_0|\mathbf{H_0}|^2 + \epsilon_r\epsilon_0|\mathbf{E_0}|^2)dV} \tag{11}$$

where the first integration is done on the bead volume ΔV, and the second one on the unperturbed cavity volume V_0. $\mathbf{E_0}$ and $\mathbf{H_0}$ are the fields of the unperturbed cavity. The constants μ_r and ϵ_r are the relative magnetic permeability and electric permittivity of the bead, respectively. Hence, pulling a dielectric bead with $\epsilon_r > 1$ and $\mu_r = 1$ means measuring the electric field only. This can be exploited during transverse movements of the bead to couple mostly with the electric field. This is the main idea behind the use of a dielectric bead for the transverse impedance measurement that will be presented in this article.

If the dielectric bead is assumed to be small enough so that the fields can be regarded as uniform for an appreciable distance behind and beyond it, the relative frequency shift can be written as

$$\frac{\Delta f}{f_R} \approx -k_{\text{SL}}\frac{|\mathbf{E_0}|^2}{U} \tag{12}$$

where k_{SL} is a constant parameter named calibration constant of the bead and it is a function only of the bead's geometry and material. U is the total stored energy in the cavity [i.e., the denominator of (11)]. However, in practical measurements, the phase shift of the transmission scattering parameter can be obtained more accurately than the frequency shift. The relationship between this phase shift and the relative frequency shift is

$$\frac{\Delta f(z)}{f_R} \approx \frac{\Delta\phi(z)\cdot(\pi/180)}{2\cdot Q_L} \tag{13}$$

where z is the location of the small perturbation, and Q_L is the loaded quality factor of the cavity.

From the frequency shift, one can compute the shunt impedance to reconstruct the beam-coupling impedance, through the following equation [27]:

$$R_S = \frac{Q_0}{2\omega_R k_{\text{SL}}}\left(\int_0^D\sqrt{\frac{|\Delta f(z)|}{f_R}}dz\right)^2 \tag{14}$$

where D is the length of the cavity, and Q_0 is the unloaded quality factor of the cavity.

B. Bead-Pull Setup and Technique

In this paragraph, the developed portable setup and the steps required to perform the bead-pull measurement of the longitudinal beam-coupling impedance are described.

1) Description of the Developed Setup: A general-purpose and portable bead-pull system has been developed and is depicted in Fig. 6. A nylon wire is stretched through the structure and held in place by two aluminum profiles with a pulley system attached. This is controlled by an Arduino-driven motor which allows the movement of the bead (glued to the nylon wire) through the cavity. A graduated scale is mounted on the two aluminum profile holders, enabling controlled transverse movements of the wire and bead. These movements are necessary for conducting transverse impedance measurements, as will be described in Section V.

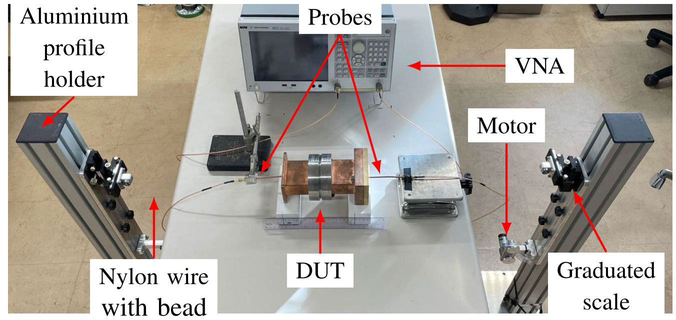

Fig. 6. Bead-pull method setup with the portable and general-purpose pulley system.

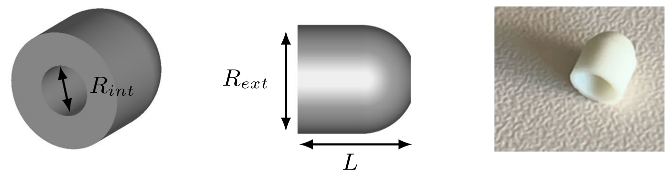

Fig. 7. Three-dimensional model of the bullet-shaped dielectric bead, a side view of it, and the real bead that was used (left to right). $L = 3.75$ mm, $R_{\text{ext}} = 1.97$ mm, $R_{\text{int}} = 0.85$ mm, and $\epsilon_r = 5.5$.

2) Bead-Pull Method for Longitudinal Impedance Measurements:

Obtaining the longitudinal beam-coupling impedance with different offsets is the starting point for the retrieval of the transverse impedance. In this section, the bead-pull method is explained in depth while showing the measurement process of the longitudinal beam-coupling impedance in the case of our DUT. The general bead-pull technique involves the following steps.

1) Calibrate the bead through simulations. Modeling the geometry of the bead in a known reference cavity, it is possible, through several simulations, to compute the frequency shift $\Delta f(z)$ by changing the longitudinal position of the bead. Furthermore, f_R, Q_0, and R_S are also output of the simulations. Finally, using the inverse of (14), it is possible to obtain the bead calibration constants k_{SL}. The dielectric bead that was used in the simulations and measurement process of our DUT is shown in Fig. 7.
   The calibration of the bead is a time-consuming process that involves multiple eigenmode simulations (all performed in CST). Primarily because the simulations must be highly accurate to resolve properly the frequency shift. In addition, the geometric modeling of the bead requires meticulous study to ensure an accurate representation.
2) Excite the resonances of the cavity and characterize them in terms of resonant frequency and quality factor with the probe method (as described in Section III-B). The results of this step are shown in Fig. 5 in the bottom plot.
3) With the probes inserted, measure the phase $\phi(z)$ of the transmission parameter S_{21} at the resonant frequency

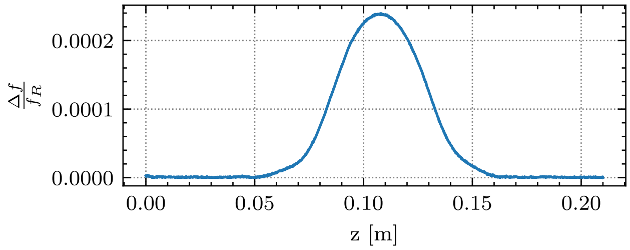

Fig. 8. Normalized Δf as a function of the longitudinal position z of the bead in the DUT.

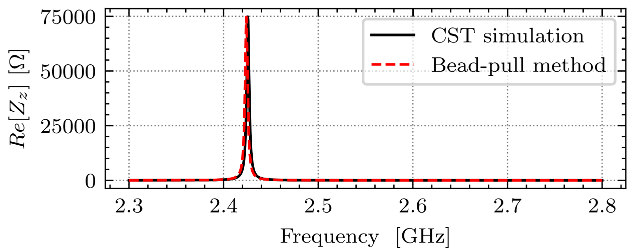

Fig. 9. Longitudinal beam-coupling impedance obtained with the bead-pull method (red curve). The expected value from CST simulations is reported as well (black curve).

while the bead is traveling inside the cavity (along the beam axis). In postprocessing, the normalized Δf is computed through (13). For the DUT, this measurement is reported in Fig. 8. It is worth mentioning that to insert the bead in the structure and to allow its transverse movements, it is required to leave the terminating waveguides open (without any measurement flange). This will introduce only a minimal perturbation on the measurements since the waveguides that are terminating the structure are chosen to have a cutoff frequency well below the fundamental cavity mode that is being characterized.

4) Compute the shunt impedance through (14).
5) Compute the longitudinal beam-coupling impedance using the resonator formula of (9).

In Fig. 9, the obtained longitudinal impedance of the DUT is depicted.

V. Transverse Beam-Coupling Impedance Measurements: A New Approach

The idea of measuring the transverse impedance by applying the bead-pull technique is inspired by the approach used in the wire method [8]. In the simple case of a device with top/bottom and left/right symmetry (which is the case for our DUT), the measured longitudinal impedance can be expanded as a power series [3], [4], [39] as follows:

$$Z_l(f) = Z_{l,0}(f) + Z_{l,1x}(f)x_0^2 + Z_{l,1y}(f)y_0^2 \quad (15)$$

where x_0 and y_0 are the transverse offsets of the source of excitation with respect to the center of the chamber (i.e., the metallic wire in the case of the wire method and the bead trajectory in the case of the bead-pull method). The first term $Z_{l,0}(f)$ is the classical longitudinal impedance (when the excitation is centered in the symmetry axis). The

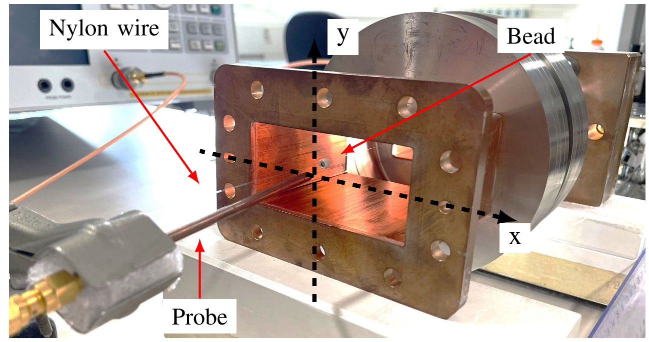

Fig. 10. Reference axis system in the structure. Offsets are given with respect to the zero, which is the center of the cavity.

frequency-dependent coefficients $Z_{l,1x}(f)$ and $Z_{l,1y}(f)$ are linked to the transverse impedance Z_x and Z_y through (8)

$$Z_x(f) = \frac{c}{2\pi f} Z_{l,1x}(f) \quad (16)$$

$$Z_y(f) = \frac{c}{2\pi f} Z_{l,1y}(f). \quad (17)$$

The new approach, in the case of the bead-pull method, consists of measuring the longitudinal impedance Z_l as a function of frequency, as described in Section IV-B2, for different transverse offsets of the bead. The offsets are given separately on the two axes by shifting the nylon wire location. This can be viewed in Fig. 10. Considering now the measured resonant frequency f_R, the related total shunt impedance R_S is a function of the bead offset with a parabolic trend [as in (15)] which can be expressed in the form

$$R_{S,x} = A \cdot x_0^2 + C \quad (18)$$

$$R_{S,y} = B \cdot y_0^2 + C \quad (19)$$

where C is the shunt impedance R_S when the bead is at the center, and A and B are the shunt impedances related to the impedance terms $Z_{l,1x}$ and $Z_{l,1y}$, respectively.

From the parabola (18) and (19), using (8), the shunt impedance related to the transverse beam-coupling impedances (on x and y) can then be obtained as follows:

$$R_{T,x} = \frac{A \cdot c}{2\pi f_R} \quad (20)$$

$$R_{T,y} = \frac{B \cdot c}{2\pi f_R}. \quad (21)$$

In the case of our DUT, measurements of $R_{S,x}$ and $R_{S,y}$ for different transverse offsets are performed. In Fig. 11, the results of measurements in the case of offsets of the dielectric bead on the x-axis is reported. The expected parabola is obtained with parameters $A \approx -66.45$ MΩ/m^2 and $C \approx$ 74.84 kΩ.

The shunt impedance related to Z_x is

$$R_{T,x} = \frac{A \cdot c}{2\pi f_R} = -1.308 \frac{\text{M}\Omega}{\text{m}}.$$

Finally, in Fig. 12, both the transverse impedances are reported and compared with the expectations coming from simulations.

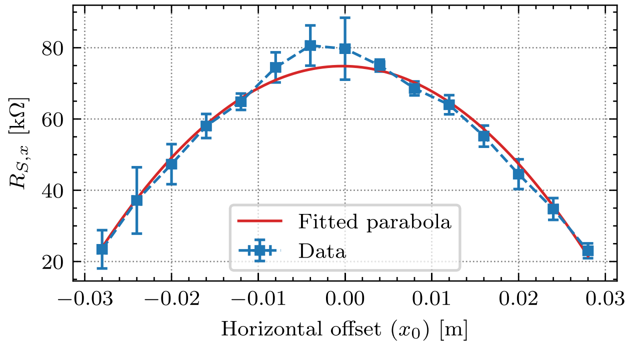

Fig. 11. $R_{S,x}$ versus x_0 offsets. The error bar was calculated from repeated measurement data. The goodness of the fit is justified by $P(\chi^2 > 5.7) = 0.93$.

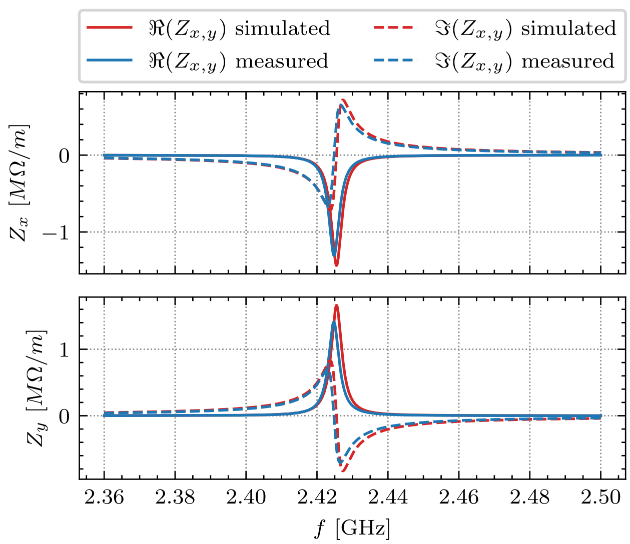

Fig. 12. Transverse beam-coupling impedances (both on x and y) obtained with the bead-pull method (blue curves). Expected values from CST simulations are reported as well (red curves).

It is possible to appreciate that not only it is possible to measure accurately the longitudinal beam-coupling impedance, but also, with the novel approach, there is also a good agreement between measurements and simulations for the transverse impedances in the general case study reported.

VI. Conclusion

In this article, a novel approach for transverse beam-coupling impedance measurements has been proposed. The new method, based on the bead-pull technique, has been described and its experimental proof-of-concept was showcased for a pillbox cavity. The method was implemented and tested developing a general-purpose, low-cost, and portable setup with the potential to be easily applied to other accelerator devices. In this article, other standard bench measurement techniques (wire method and probe method) were introduced to underline their limitations when applied to resonant structures. The setup used allowed for accurate measurements of the longitudinal beam-coupling impedance, overcoming the limitations of the existing methods. Moreover, the idea of using a dielectric bead, which couples with the electric field when giving a transverse offset to the bead, allowed to measure the longitudinal impedance in several transverse locations. This, combined with the Panofsky–Wenzel theorem, proved the possibility of measuring the transverse beam-coupling impedance by adopting the bead-pull technique. The results on the pillbox cavity showed an excellent agreement with the expected values from simulations. Minimal disagreement can be explained by the absence of the flanges closing the structure.

References

[1] G. Apollinari, O. Brüning, T. Nakamoto, and L. Rossi. (2015). *High Luminosity Large Hadron Collider HL-LHC*. [Online]. Available: https://cds.cern.ch/record/2120673

[2] G. Arduini et al., "High luminosity LHC: Challenges and plans," *J. Instrum.*, vol. 11, Dec. 2016, Art. no. C12081.

[3] A. W. Chao, *Physics of Collective Beam Instabilities in High Energy Accelerators* (Wiley Series in Beam Physics and Accelerator Technology). Hoboken, NJ, USA: Wiley, 1993.

[4] L. Palumbo, V. G. Vaccaro, and M. Zobov, *Wake Fields and Impedance*, document LNF/94/041, 1994.

[5] C. Zannini, G. Rumolo, and G. Iadarola, "Power loss calculation in separated and common beam chambers of the LHC," in *Proc. 5th Int. Part. Accel. Conf.*, Jul. 2014, pp. 1–4.

[6] E. Metral, G. Rumolo, and W. Herr, *Impedance and Collective Effects*. Cham, Switzerland: Springer, 2020, pp. 105–181, doi: 10.1007/978-3-030-34245-6_4.

[7] V. R. Marrazzo et al., "Experimental tests of a full analog fiber optic monitoring system suitable for safety application at CERN," *IEEE Trans. Instrum. Meas.*, vol. 72, pp. 1–8, 2023.

[8] A. Mostacci et al., "Rf coupling impedance measurements for particle accelerator devices," in *Proc. 20th IMEKO TC-4 Int. Symp. Res. Elect. Electronic Meas. Economic Upturn*, Jan. 2014, pp. 80–85.

[9] V. G. Vaccaro, *Coupling Impedance Measurements: An Improved Wire Method*, document INFN/TC-94/023, 1994, pp. 1049–1052.

[10] G. Di Massa and M. R. Masullo, "Beam impedance measurements-coaxial wire method," in *Proc. Conf. Rec. IEEE Part. Accel. Conf.*, May 1991, pp. 789–791.

[11] M. R. Masullo, V. G. Vaccaro, and M. Panniello, "The stretched wire method: A comparative analysis performed by means of the mode matching technique," in *Proc. Linear Accel. Conf.*, 2010, pp. 932–934.

[12] F. Argan, F. Console, M. Migliorati, L. Palumbo, and S. De Santis, "Measurements of the longitudinal impedance of a coaxial cavity coupled with a circular pipe through slots," in *Proc. 7th Eur. Part. Accel. Conf.*, Jun. 2000, pp. 1426–1428.

[13] R. Wegner, W. Wuensch, G. Burt, and B. Woolley, "Bead-pull measurement method and tuning of a prototype CLIC crab cavity," in *Proc. 27th Int. Linear Accel. Conf.*, 2014, pp. 1–3.

[14] L. Palumbo, A. Mostacci, R. Re, L. Ficcadenti, D. Alesini, and B. Spataro. (2009). *About Non Resonant Perturbation Field Measurement in Standing Wave Cavities*. [Online]. Available: https://api.semanticscholar.org/CorpusID

[15] A. Wolski, *Beam Dynamics in High Energy Particle Accelerators*. London, U.K.: Imperial College Press, 2014. [Online]. Available: https://www.worldscientific.com/doi/abs/10.1142/p899

[16] B. Salvant et al., "Beam induced RF heating in LHC in 2015," in *Proc. 7th Int. Part. Accel. Conf.*, 2015, pp. 602–605.

[17] F. Fienga et al., "Direct measurement of beam-induced heating on accelerator pipes with fiber optic sensors: Numerical analysis validation," *IEEE Trans. Instrum. Meas.*, vol. 72, pp. 1–9, 2023.

[18] W. K. H. Panofsky and W. A. Wenzel, "Some considerations concerning the transverse deflection of charged particles in radio-frequency fields," *Rev. Sci. Instrum.*, vol. 27, no. 11, p. 967, Nov. 1956.

[19] D. Pozar, *Microwave Engineering*, 3rd ed., Hoboken, NJ, USA: Wiley, 2009. [Online]. Available: https://books.google.ch/books?id=UZgvwJ3Eex8C

[20] E. Jensen. (Sep. 2014). *RF Cavity Design*. Comments: 25 Pages, Contribution CAS—CERN Accel. School, Adv. Accel. Phys. Course, Trondheim, Norway, Trondheim, Norway. [Online]. Available: https://cds.cern.ch/record/1982429

[21] K. Y. Ng, *Physics of Intensity Dependent Beam Instabilities*. Singapore: World Scientific, 2005. [Online]. Available: https://www.worldscientific.com/doi/abs/10.1142/5835

[22] *Cern Pyheadtail Macro-Particle Code for Simulating Beam Dynamics in Particle Accelerators With Collective Effects*. [Online]. Available: https://github.com/PyCOMPLETE/PyHEADTAIL

[23] N. Mounet. (2014). *DELPHI: An Analytic Vlasov Solver for Impedance-Driven Modes*. [Online]. Available: http://cds.cern.ch/record/1954277

[24] L. Sito et al., "A Python package to compute beam-induced heating in particle accelerators and applications," in *Proc. ICFA Adv. Beam Dyn. Workshop High-Intensity High-Brightness Hadron Beams*, Geneva, Switzerland, Apr. 2024, pp. 611–614. [Online]. Available: https://jacow.org/hb2023/papers/thbp52.pdf

[25] P. Krkotić et al., "Limitations from LHC RF fingers," in *Proc. 15th Int. Part. Accel. Conf.*, pp. 947–950.

[26] C. Zannini et al., "Impedance and thermal studies of the cern sps wirescanners and mitigation of wire heating," in *Proc. 15th Int. Part. Accel. Conf.*, pp. 2260–2263.

[27] D. M. F. El Dali, G. De Michele, S. Fanella, E. Métral, and C. Zannini, "Numerical calibration of the bead-pull setup for beam coupling impedance evaluation," in *Proc. 15th Int. Part. Accel. Conf.*, 2022, pp. 607–609.

[28] F. Caspers, "Beam impedance measurements using the coaxial wire method," CERN, Geneva, Switzerland, Tech. Rep., CM-P00059158, 1988.

[29] G. Nassibian and F. Sacherer, "Methods for measuring transverse coupling impedances in circular accelerators," *Nucl. Instrum. Methods*, vol. 159, no. 1, pp. 21–27, Feb. 1979.

[30] E. L. N. Jensen. (2000). *An Improved Log-Formula for Homogeneously Distributed Impedance*. [Online]. Available: https://api.semanticscholar.org/CorpusID

[31] F. Caspers, A. Mostacci, and H. Tsutsui. (2000). *Impedance Evaluation of the Sps Mke Kicker With Transition Pieces Between Tank and Kicker Module*. [Online]. Available: https://api.semanticscholar.org/CorpusID

[32] T. Kroyer, E. Gaxiola, and F. Caspers. (2007). *Longitudinal and Transverse Wire Measurements for the Evaluation of Impedance Reduction Measures on the MKE Extraction Kickers*. [Online]. Available: https://api.semanticscholar.org/CorpusID

[33] V. Vlachodimitropoulos, M. Barnes, A. Chmielinska, and L. Ducimetière, "Transverse impedance measurements and simulations of the LHC injection kicker magnet," in *Proc. 10th Int. Part. Accel. Conf. (IPAC)*, Melbourne, NSW, Australia. Geneva, Switzerland: JACoW, Jun. 2019, pp. 3986–3989. [Online]. Available: http://jacow.org/ipac2019/papers/thprb075.pdf

[34] B. Salvant, N. Mounet, and C. Zannini. (2010). *Quadrupolar Transverse Impedance of Simple Models of Kickers*. [Online]. Available: https://api.semanticscholar.org/CorpusID

[35] C. Antuono, M. Migliorati, A. Mostacci, and C. Zannini, "A wireless method for beam coupling impedance measurements of the LHC goniometer," in *Proc. 68th Adv. Beam Dyn. Workshop High-Intensity High-Brightness Hadron Beams*, Apr. 2024, pp. 407–410. [Online]. Available: https://jacow.org/hb2023/papers/thafp05.pdf

[36] D. Systèmes. *CST Studio Suite*. Accessed: Apr. 23, 2024. [Online]. Available: https://www.3ds.com/products/simulia/cst-studio-suite

[37] R. E. Collin, *Foundations for Microwave Engineering* (Series on Electromagnetic Wave Theory), 2nd ed., Piscataway, NJ, USA: IEEE Press, 2001.

[38] L. C. Maier and J. C. Slater, "Field strength measurements in resonant cavities," *J. Appl. Phys.*, vol. 23, no. 1, pp. 68–77, Jan. 1952. [Online]. Available: https://api.semanticscholar.org/CorpusID:123235264

[39] S. Heifets, A. Wagner, and B. Zotter, "Generalized impedances and wakes in asymmetric structures," Stanford Linear Accel. Center, Stanford Univ., CA, USA, Tech. Rep. SLAC/AP110, Jan. 1998.

Chiara Antuono received the M.Sc. degree in electronics engineering from Sapienza University of Rome, Rome, Italy, in 2021, where she is currently pursuing the Ph.D. degree in physics of particle accelerators.

She is currently with Accelerator and Beam Physics Section, European Organization for Nuclear Research (CERN), Geneva, Switzerland. During her studies at CERN, she has further developed expertise in applied electromagnetism, electromagnetic simulations, and beam-coupling impedance measurements. Her research focuses primarily on beam-coupling impedance and collective effects.

Leonardo Sito received the B.Sc. and M.Sc. degrees in electronics engineering from the University of Naples Federico II, Naples, Italy, in 2019 and 2022, respectively, where he is currently pursuing the Ph.D. degree in information technology and electrical engineering.

As part of his doctoral studies, he is a member of the Doctoral Student Program with Accelerator and Beam Physics Section, European Organization for Nuclear Research (CERN), Geneva, Switzerland. His research focuses on beam-coupling impedance and the use of metamaterials as potential mitigation strategies. His areas of expertise include electromagnetic and thermal simulations and measurements of high-energy physics devices.

Eleonora Calzone received the bachelor's degree in physics from the Sapienza University of Rome, Rome, Italy, in 2022, where she is currently pursuing the master's degree in physics, with a focus on fundamental interactions.

In the summer of 2023, she participated in the prestigious Summer Student Program at European Organization for Nuclear Research (CERN), Geneva, Switzerland, where she collaborated with the Accelerator and Beam Physics Group on bench beam impedance measurements, further enhancing her expertise in accelerator physics. Her main research area is particle physics and she is particularly interested in accelerator physics.

D. el Dali, photograph and biography not available at the time of publication.

Mauro Migliorati has been a Supervisor of several Ph.D. Students of accelerator physics. He is a Full Professor of applied physics with the University of Rome La Sapienza, Rome, Italy. He is a Member of the Board of the Joint University Accelerator School (JUAS), where he has been teaching a course on "Space Charge and Instabilities," since 2010. He collaborates with the Italian National Institute of Nuclear Physics (INFN), Rome, and European Organization for Nuclear Research (CERN), Geneva, Switzerland, on themes related to both circular and linear accelerators. He is responsible for the impedance budget and collective effects of the Future Circular Collider Project—FCC-ee. He has co-authored more than 250 articles in the field of particle accelerators. His research activity regards accelerator physics, particularly beam dynamics and collective effects.

Andrea Mostacci received the degree (Hons.) in electronic engineering from Sapienza University of Rome, Rome, Italy, in 1997, and the Ph.D. degree in applied electromagnetism from the Sapienza University of Rome, Italy, Rome, in 2001.

He started his career in the field of engineering of particle accelerators at European Organization for Nuclear Research (CERN), Geneva, Switzerland. He is currently an Associate Professor in physics at Sapienza Teaching Electromagnetism, Microwave Measurements and Accelerator Physics. In 2002, he founded the Advanced Particle Accelerator Laboratory, Sapienza. He has co-authored more than 270 publications. His research interests include beam–wall interaction in accelerators, coupling impedance and WFs, design and measurements of RF devices for beam diagnostics and manipulation, high brightness photoinjectors for free electron lasers and radiation sources, laser–plasma interaction for particle acceleration, terahertz sources, and medical and industrial application of particle accelerators.

Francesco Fienga (Member, IEEE) received the M.Sc. degree in physics and the Ph.D. degree in information technology and electrical engineering from the Università degli Studi di Napoli Federico II, Naples, Italy, in 2013 and 2017, respectively.

Currently, he is an Assistant Professor of electronics with the Department of Electrical Engineering and Information Technology, Università degli Studi di Napoli Federico II. He is a member of CMS at European Organization for Nuclear Research (CERN). His research focus lies in the areas of fiber optic sensors and optoelectronic devices.

Vincenzo Romano Marrazzo received the B.Sc. and M.Sc. degrees in electronics engineering and the Ph.D. degree in information technology and electrical engineering from the University of Naples Federico II, Naples, Italy, in 2014, 2017, and 2021, respectively.

He is currently a Researcher with the Department of Electrical Engineering and Information Technology, University of Naples Federico II. His research field comprises design and development of electronic and optoelectronic systems for the reading of sensors in normal and harsh environments.

Dr. Marrazzo is a member of CMS collaboration at European Organization for Nuclear Research (CERN) (CH).

Giovanni Breglio received the degree (cum laude) in electronic engineering from the University of Naples Federico II, Naples, Italy, in 1990, and the Ph.D. degree in electronic engineering and computer science from the University of Naples Federico II, in 1994.

He is a Full Professor of electronics with the University of Naples Federico II. He is a Co-ordinator with the OptoPower Laboratory, DIETI Department. He has authored more than 90 peer-reviewed journal articles and about 170 proceedings of international conferences. His research interests include electro-thermal modeling and characterization of semiconductor devices, development and design of new fiber optical sensors and monitoring systems, and design of silicon-based optoelectronic devices.

Dr. Breglio is a member of CMS Collaboration at European Organization for Nuclear Research (CERN) (CH), for the UNINA-DIET@CMS, as a Team Leader. In 2023, he has been the Co-General Chair and a TCP Member of the International Conference ICSCRM'23. He is the Trach-Chair into the TCP of ESREF'24 International Conference.

G. Rumolo, photograph and biography not available at the time of publication.

Carlo Zannini received the degree in electronic engineering from the University of Naples Federico II. Naples, Italy, in 2008, and the Ph.D. degree in physics from Ecole Polytechnique Federale de Lausanne, Lausanne, Switzerland, in 2013.

In 2008, he was a Student at European Organization for Nuclear Research (CERN), Geneva, Switzerland, and in 2015, he left CERN to join Applications of Detectors and Accelerators to Medicine (ADAM), as a Senior RF Engineer. He returned to CERN, in 2018, as a Staff Accelerator Physicist, continuing his research on impedance and its associated effects, where he is an Accelerator Physicist. With over 15 years of experience in electromagnetic field theory, simulations, and measurements, he is specialized in beam-coupling impedance and related effects, such as beam-induced heating and coherent instabilities.